Journal of Physics: Conference Series **163** (2009) 012052 doi:10.1088/1742-6596/163/1/012052

STUDIES OF X-RAY PRODUCTION FOLLOWING CHARGE EXCHANGE RECOMBINATION BETWEEN HIGHLY CHARGED IONS AND NEUTRAL ATOMS AND MOLECULES

G. V. Brown[†], P. Beiersdorfer[†], H. Chen[†], J. Clementson[†], M. Frankel[†], M. F. Gu[†], R. L. Kelley[♯], C. A. Kilbourne[♯], F. S. Porter[♯], D. B. Thorn[†], B. J. Wargelin[‡]

[†]Lawrence Livermore National Laboratory, Livermore, CA 94550
[♯]NASA/Goddard Space Flight Center, Greenbelt, MD 20770
[‡]Harvard-Smithsonian Center for Astrophysics, Cambridge, MA 02138

E-mail: gregbrown@llnl.gov

Abstract. We have used microcalorimeters built by the NASA/Goddard Space Flight Center and the Lawrence Livermore National Laboratory SuperEBIT electron beam ion trap to measure X-ray emission produced by charge exchange reactions between highly charged ions colliding with neutral helium, hydrogen, and nitrogen gas. Our measurements show the spectral dependence on neutral species and also show the distinct differences between spectra produced by charge exchange reactions and those produced by direct electron-impact excitation. These results are part of an ongoing experimental investigation at the LLNL SuperEBIT facility of charge exchange spectral signatures and can be used to interpret X-ray spectra produced by a variety of laboratory and celestial sources including cometary and planetary atmospheres, the Earth's magnetosheath, the heliosphere, and tokamaks.

The radiationless transfer of one or more electrons to a projectile ion from a target neutral atom or molecule is known as charge exchange recombination (CX). Photon emission is produced by CX when the transferred electron is captured into an excited state and that state radiatively decays. CX plays an important role in a variety of plasmas and is believed to be a significant X-ray line formation process in many non-equilibrium astrophysical objects. For example, X-ray emission from CX has been identified or hypothesized as a source of X-ray production in planetary atmospheres, including the aurora of Jupiter [1, 2] and the Earth's magnetosheath [3], supernova remnants [4], and the galactic center and ridge [4, 5]. CX is also believed to contribute significantly to the cosmic soft X-ray background. In addition, CX produces a significant amount of radiation in some laboratory plasmas, such as during neutral beam heating in tokamak plasmas. Identification and interpretation of the X-ray spectral signatures from charge exchange in complex sources, however, has been challenging because little targeted laboratory data are available, and while in some cases agreement between theory and measurement is good [6], in many significant discrepancies still exist [7, 8, 9]. To help better understand charge exchange

© 2009 IOP Publishing Ltd

recombination and to provide benchmarks for theory, we have used the SuperEBIT electron beam ion trap (EBIT) facility at Lawrence Livermore National Laboratory (LLNL) and a NASA/Goddard Space Flight Center microcalorimeter instrument to measure the X-ray spectral signatures of charge exchange. Here we present a brief description of the measurement technique and selected results.

The LLNL EBIT facility, home of the original EBIT [10, 11], is well tested and has been used in numerous atomic physics and laboratory astrophysics experiments. Most basically, it consists of an electron beam, compressed by a 3 Tesla magnetic field, that creates and excites ions, and a trap region defined by three drift tubes that confine the ions along the axis of the electron beam. The LLNL EBIT can operate in two modes: the electron trapping mode, and the magnetic trapping mode [12]. In the magnetic trapping mode, the electron beam is turned off and the ions are trapped radially by the 3 Tesla magnetic field. This differs from the electron trapping mode, most often used in EBIT experiments, where the beam is on and the ions are trapped radially by the potential created by the electron beam's space charge. For CX experiments, EBIT is operated in a phase that includes both trapping modes. Ions are created in the electron trapping mode, then the X-ray emission from CX is measured in the magnetic trapping mode. Neutral targets are introduced continuously throughout the EBIT phase using a ballistic gas injector. Figure 1 shows a typical EBIT phase diagram denoting the electron and magnetic trapping modes and the spectra acquired during each mode.

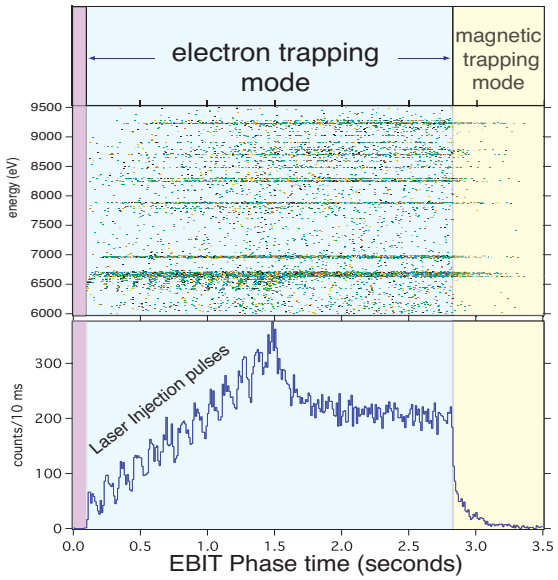

Figure 1. Energy (upper frame) and total counts (lower frame) versus EBIT phase time. The electron and magnetic trapping mode portions of the phase are both shown. The X-ray emission from charge exchange between highly charged Fe ions and N_2 takes place during the magnetic trapping mode. For this experiment, Fe was injected into EBIT using a laser ablation injection system [13]. Each of the laser injection pulses can be seen in both frames. Between 0 and 0.1 seconds the ions are dumped from the trap and no X-ray emission occurs.

For these experiments, photons were detected using one of the microcalorimeter instruments developed and built at the NASA/Goddard Space Flight Center [14, 15] and operated at LLNL. In particular, the second generation XRS/EBIT was used[1]. The XRS/EBIT has an energy

[1] For a more complete description of the microcalorimeter instruments operated at the LLNL EBIT facility, see Porter et al. these proceedings.

resolution of $5-6$ eV at 6 keV and is able to measure time-resolved spectra. Time resolution is necessary in order to "cut out" the electron trapping mode portion of the EBIT phase so that the X-ray spectra produced solely by charge exchange can be analyzed separately. High energy resolution is necessary to resolve high-n Rydberg states (see below).

Figures 2 and 3 show spectra produced by charge exchange between hydrogenic Fe^{25+} and bare Fe^{26+} projectiles and neutral H_2, N_2, and He targets producing X-ray emission from helium-like Fe^{24+} and hydrogenic Fe^{25+}, respectively. Figure 2 shows the He-like Fe^{24+} spectrum produced by CX compared to the spectrum from Fe^{24+} produced by direct electron impact excitation. In the CX case, the 1s2s $^3S_1 \rightarrow 1s^2\ ^1S_0$ forbidden line "z" is much stronger than the 1s2p $^1P_1 \rightarrow 1s^2\ ^1S_0$ resonance line "w", in stark contrast to the case of direct electron impact excitation. This well known spectral signature [4, 6, 8] can be used to identify the presence of CX as an X-ray production mechanism, even using a relatively low-resolution spectrometer, such as a CCD or germanium detector [16, 17].

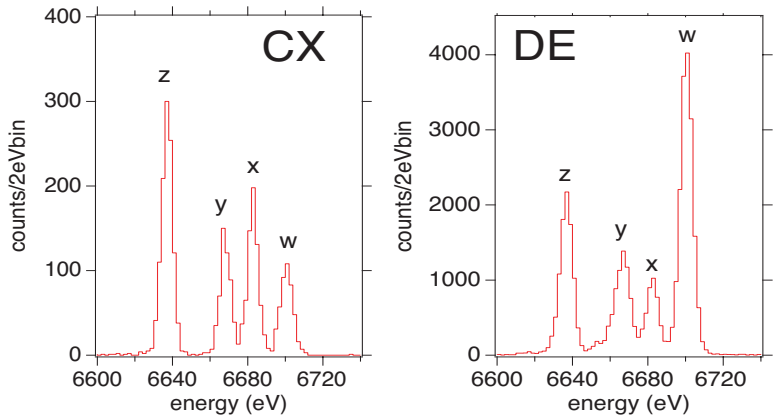

Figure 2. Comparsion of X-ray emission from helium-like Fe^{24+} produced by charge exchange (CX) between hydrogenic Fe^{25+} and N_2 and produced by direct electron impact excitation (DE).

Figure 3 compares the high-n Rydberg X-ray lines produced by CX between Fe^{26+} and neutral H_2, N_2, and He. Note that the strongest X-ray line in the case of He is $n_{max} = 12 \rightarrow 1$, while in the case of H_2 and N_2 it is n_{max}=14 $\rightarrow$ 1. The lower n_{max} for the He targets is caused by the fact that the principal quantum number, n, of the state of the ion with the maximum capture cross section depends on the ionization potential of the neutral material [4]. Although these results do follow the trend predicted by theory, i.e., n_{max} decreases as the ionization potential of the neutral target increases, the measured n_{max} is about 2 levels higher than predicted by the usual scaling formula. Our results show that, given high enough energy resolution, CX spectra can be used to distinguish among neutral target material.

Significant advances have been made in understanding the X-ray production from CX; however, much work remains to fully realize its diagnostic potential, particularly in the case of charge exchange with L-shell ions [18, 19]. Studies of CX will be especially useful in the analysis of data acquired by future satellite missions, such as Astro-H, which will carry a microcalorimeter similar to the one used in these experiments, and that will for the first time provide high resolution, high signal-to-noise spectra of extended sources.

Acknowledgments

Part of this work was performed under the auspices of the U. S. Department of Energy by Lawrence Livermore National Laboratory under Contract DE-AC52-07NA27344 and is also supported by NASA grants to LLNL, SAO, Stanford University, and the NASA/GSFC.

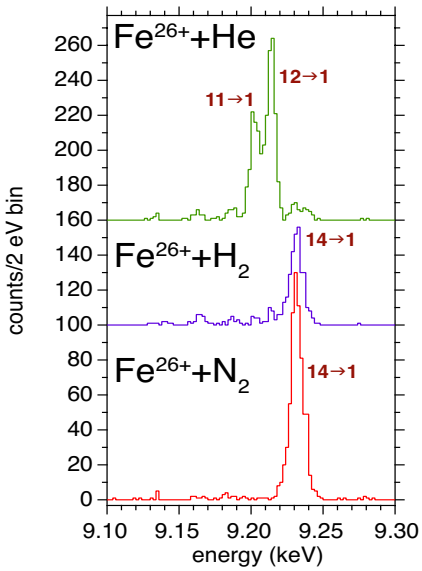

Figure 3. Comparison of X-ray emission from high-n $\rightarrow$ 1 Rydberg transitions following CX between bare Fe^{26+} and He, H_2, and N_2. The ionization potential for He, H_2, and N_2 are 24.6 eV, 15.4 eV, and 15.6 eV, respectively. The predicted value for n for the state of maximum capture for the He targets is 9, and for H_2, and N_2 is 12 or 13. The collision energy for these reactions is $\approx$ 10 eV/amu.

References

[1] Gladstone G R, Waite J H, Grodent D, Lewis W S, Crary F J, Elsner R F, Weisskopf M C, Majeed T, Jahn J M, Bhardwaj A, Clarke J T, Young D T, Dougherty M K, Espinosa S A and Cravens T E 2002 **415** 1000
[2] Elsner R F, Lugaz N, Waite J H, Cravens T E, Ford P, Grodent D, Bhardwaj A, Macdowell R J, Desch M D and Majeed T
[3] Fujimoto R, Mitsuda K, Mccammon D, Takei Y, Bauer M, Ishisaki Y, Porter S F, Yamaguchi H, Hayashida K and Yamasaki N Y 2007 *pasj* **59** 133–140
[4] Wargelin B J, Beiersdorfer P and Brown G V 2008 *Can. J. Phys.* **86** 151–169
[5] Beiersdorfer P, Bitter M, Marion M and Olson R E 2005 *pra* **72** 032725–+
[6] Beiersdorfer P, Olson R E, Brown G V, Chen H, Harris C L, Neill P A, Schweikhard L, Utter S B and Widmann K 2000 *Phys. Rev. Lett.* **85** 5090
[7] Beiersdorfer P, Lisse C M, Olson R E, Brown G V and Chen H 2001 *Astrophys. J. Lett.* **549** L147 – L150
[8] Otranto S, Olson R and beiersdorfer P 2008 *Can. J. Phys.* **86** 171–174
[9] Beiersdorfer P 2008 *Can. J. Phys.* **86** 1–10
[10] Marrs R 2008 *Can. J. Phys.* **86** 11–18
[11] Beiersdorfer P, Schweikhard L, López-Urrutia J C and Widmann K 1996 *Rev. Sci. Instrum.* **67** 3818–3826
[12] Niles A M, Magee E W, Thorn D B, Brown G V, Chen H and Beiersdorfer P 2006 *rsi* **77**
[13] Porter F S, Beiersdorfer P, Boyce K R, Brown G V, Chen H, Gygax J, Kahn S M, Kelley R L, Kilbourne C A, Magee E and Thorn D B 2008 *Can. J. Phys.* **86** 231–240
[14] Porter F S, Beiersdorfer P, Boyce K R, Brown G V, Chen H, Kelley R L and Kilbourne C A 2004 *Rev. Sci. Instrum.* **75** 3772
[15] Koyama K, Hyodo Y, Inui T, Nakajima H, Matsumoto H, Tsuru T G, Takahashi T, Maeda Y, Yamazaki N Y, Murakami H, Yamauchi S, Tsuboi Y, Senda A, Kataoka J, Takahashi H, Holt S S and Brown G V 2007 *pasj* **59** 245–255
[16] Wargelin B J, Beiersdorfer P, Neill P A, Olson R E and Scofield J H 2005 *apj* **634** 687–697